View metadata, citation and similar papers at core.ac.uk

brought to you by CORE

provided by Harvard University - DASH

DIGITAL ACCESS TO SCHOLARSHIP AT HARVARD

Depletion of RUNX1/ETO in t(8;21) AML cells leads to genome-wide changes in chromatin structure and transcription factor binding

The Harvard community has made this article openly available. Please share how this access benefits you. Your story matters.

Citation	Ptasinska, A, S A Assi, D Mannari, S R James, D Williamson, J Dunne, M Hoogenkamp, et al. 2012. Depletion of RUNX1/ETO in t(8;21) AML cells leads to genome-wide changes in chromatin structure and transcription factor binding. Leukemia 26(8): 1829-1841.
Published Version	doi:10.1038/leu.2012.49
Accessed	February 19, 2015 10:49:32 AM EST
Citable Link	http://nrs.harvard.edu/urn-3:HUL.InstRepos:10471527
Terms of Use	This article was downloaded from Harvard University's DASH repository, and is made available under the terms and conditions applicable to Other Posted Material, as set forth at http://nrs.harvard.edu/urn-3:HUL.InstRepos:dash.current.terms-of-use#LAA

(Article begins on next page)

Open

Leukemia (2012) **26**, 1829 – 1841
© 2012 Macmillan Publishers Limited All rights reserved 0887-6924/12
www.nature.com/leu

ORIGINAL ARTICLE

Depletion of RUNX1/ETO in t(8;21) AML cells leads to genome-wide changes in chromatin structure and transcription factor binding

A Ptasinska[1,2,8], SA Assi[3,8], D Mannari[4,9], SR James[1,9], D Williamson[5], J Dunne[4], M Hoogenkamp[1], M Wu[6], M Care[1], H McNeill[5], P Cauchy[2], M Cullen[1], RM Tooze[1], DG Tenen[6,7], BD Young[4], PN Cockerill[1,2], DR Westhead[3], O Heidenreich[5] and C Bonifer[1,2]

The t(8;21) translocation fuses the DNA-binding domain of the hematopoietic master regulator RUNX1 to the ETO protein. The resultant RUNX1/ETO fusion protein is a leukemia-initiating transcription factor that interferes with RUNX1 function. The result of this interference is a block in differentiation and, finally, the development of acute myeloid leukemia (AML). To obtain insights into RUNX1/ETO-dependant alterations of the epigenetic landscape, we measured genome-wide RUNX1- and RUNX1/ETO-bound regions in t(8;21) cells and assessed to what extent the effects of RUNX1/ETO on the epigenome depend on its continued expression in established leukemic cells. To this end, we determined dynamic alterations of histone acetylation, RNA Polymerase II binding and RUNX1 occupancy in the presence or absence of RUNX1/ETO using a knockdown approach. Combined global assessments of chromatin accessibility and kinetic gene expression data show that RUNX1/ETO controls the expression of important regulators of hematopoietic differentiation and self-renewal. We show that selective removal of RUNX1/ETO leads to a widespread reversal of epigenetic reprogramming and a genome-wide redistribution of RUNX1 binding, resulting in the inhibition of leukemic proliferation and self-renewal, and the induction of differentiation. This demonstrates that RUNX1/ETO represents a pivotal therapeutic target in AML.

Leukemia (2012) **26,** 1829 – 1841; doi:10.1038/leu.2012.49

Keywords: acute myeloid leukemia; RUNX1/ETO; epigenetic regulation; chromatin; integrated analysis of high-throughput data

INTRODUCTION

Chromosomal rearrangements are a hallmark of hematopoietic malignancies. Many of these translocations generate aberrant transcriptional regulators that reproducibly lead to defined blocks in differentiation.[1] A subclass of acute myeloid leukemia (AML) is associated with a group of chromosomal translocations that each result in disruption of the function of the core factor-binding (CBF) complex, which consists of a heterodimer of RUNX transcription factor family members and their binding partner CBFβ.[2] The best-characterized CBF-type translocation is t(8;21), which fuses *RUNX1* (*AML1*), a gene that is essential for normal hematopoiesis,[3] with the gene encoding transcriptional co-repressor *ETO* (*RUNX1T1* or *MTG8*).[4,5] The ectopic expression of RUNX1/ETO redirects the specific gene expression program of normal precursor cells.[6] The mechanism of such deregulation is based on RUNX1/ETO interfering with normal RUNX1 function.[7-11] However, the molecular details of this interference are poorly understood on a genome-wide level. Several studies have demonstrated that RUNX1/ETO acts as a constitutive repressor by recruiting histone deacetylase complexes, and that it interferes directly with other transcriptional regulators of hematopoiesis such as C/EBPα.[12-16] The presence of RUNX1/ETO can alternatively lead to gene activation.[17-20]

The t(8;21) translocation is a leukemia-initiating event, and fusion gene sequences can be found long before the onset of leukemia in the blood from newborn children.[21] However, the induction of fully developed AML in t(8;21) patients requires secondary genetic alterations,[22-25] which complicates the establishment of *in vitro* model systems for gain-of-function studies. In order to evaluate the suitability of RUNX1/ETO as a therapeutic target, it is therefore necessary to identify its target sites at the genome-wide level in actual leukemic cells, to define its individual role in reprogramming gene expression networks and to determine whether its continued presence is required for maintaining deregulation. As RUNX1/ETO and RUNX1 occupy the same binding sites, it is also important to elucidate how chromatin and RUNX1 occupancy respond to loss of RUNX1/ETO binding at its target genes.

To this end, we determined genome-wide patterns of RUNX1/ETO occupancy in primary cells from patients and t(8;21) cell lines, and compared histone acetylation profiles, RNA-Polymerase II occupancy, RUNX1 binding and gene expression before and after siRNA-mediated depletion of RUNX1/ETO. Global loss of RUNX1/ETO binding results in widespread and complex changes in chromatin structure patterns, RUNX1 occupancy and

[1]Section of Experimental Haematology, Leeds Institute of Molecular Medicine, University of Leeds, Leeds, UK; [2]School of Cancer Sciences, Institute of Biomedical Research, College of Medical and Dental Sciences, University of Birmingham, Birmingham, UK; [3]Faculty of Biological Sciences, University of Leeds, Leeds, UK; [4]Barts Cancer Institute, Queen Mary University of London, London, UK; [5]Northern Institute of Cancer Research, University of Newcastle, Newcastle upon Tyne, UK; [6]Cancer Science Institute, National University of Singapore, Singapore, Singapore and [7]Harvard Stem Cell Institute, Harvard Medical School, Boston, MA, USA. Correspondence: Professor C Bonifer, School of Cancer Sciences, Institute of Biomedical Research, College of Medical and Dental Sciences, University of Birmingham, Birmingham B15 2TT, UK.
E-mail: c.bonifer@bham.ac.uk
or Dr O Heidenreich, Northern Institute of Cancer Research, University of Newcastle, Paul O'Gorman Building, Framlington Place, Newcastle upon Tyne NE2 4HH, UK.
E-mail: olaf.heidenreich@ncl.ac.uk
[8]These authors contributed equally to this work.
[9]These authors contributed equally to this work.
Received 14 February 2012; accepted 15 February 2012; accepted article preview online 20 February 2012; advance online publication, 16 March 2012

gene expression, indicating that RUNX1/ETO-mediated transcriptional reprogramming is amenable to therapeutic intervention.

MATERIALS AND METHODS

Human primary cells and cell lines

Patient material was obtained with the required ethical approval from the NHS Research Ethics Committees (Leeds Teaching Hospitals NHS Trust and Newcastle upon Tyne Hospitals NHS Foundation Trust) or with informed consent from adult patients at St Bartholomew's Hospital, London.

The Kasumi-1 cell line was obtained from the DSMZ cell line repository (http://www.dsmz.de/) and was cultured in RPMI1640 containing 10% fetal calf serum. SKNO-1 cells were maintained in RPMI1640 supplemented with 20% FCS and 7 ng/ml granulocyte–macrophage colony-stimulating factor. RAW264.7 cells were cultured in Dulbecco's modified Eagle's Medium containing 10% fetal calf serum.

siRNA transfections

Kasumi-1 and SKNO-1 cells and AML blasts were transfected with 200 nM of siRNA using a Fischer EPI 3500 electroporator (Fischer, Heidelberg, Germany) as described previously.[26] For time course experiments, sequential siRNA electroporations were performed at days 0, 4 and 7. The following siRNAs were used: RUNX1/ETO siRNA (sense, 5′-CCUCGAAAU CGUACUGAGAAG-3′; antisense, 5′-UCUCAGUACGAUUUCGAGGUU-3′), mismatch control siRNA (sense, 5′-CCUCGAAUUCGUUCUGAGAAG-3′; antisense, 5′-UC UCAGAACGAAUUCGAGGUU-3′).

RNA and protein isolation, real-time PCR and western blotting

RNA was isolated 2, 4, 7 and 10 days after siRNA electroporation using RNeasy columns (Qiagen, Hilden, Germany). Total protein was precipitated by adding two volumes of acetone to the flow through of the RNeasy columns and then resuspended in urea buffer (9 M urea, 4% (w/w) 3-((3-cholamidopropyl)-dimethylammonio)-propanesulphonate, 1% (w/w) dithiothreitol). Reverse transcription, real-time PCR and western blotting were performed as described.[27]

Chromatin immunoprecipitation

Chromatin immunoprecipitation (ChIP) was performed using the following antibodies: ETO (C-terminus-specific, Santa Cruz Biotechnology, Wembley, UK, sc-9737X), RUNX1 (C-terminus-specific, Abcam, Cambridge, UK, ab23980), RNA-Polymerase II phospho S2 (ab5095) and H3K9Ac (ab4441).

DNase I hypersensitive site mapping

Genome-wide hypersensitive sites were mapped as described in Leddin *et al*.[28]

Library generation and sequencing

Libraries of DNA fragments from ChIP or DNase I treatment were prepared from ~10 ng of DNA using standard procedures. DNA libraries were subject to massively parallel DNA sequencing on an Illumina Genome Analyzer (Illumina, Little Chesterford, UK).

Luciferase reporter assay

Reporter constructs were generated in the pGL4-Basic plasmid with promoter sequences or in the pGL4-TK plasmid (Promega, Southampton, UK) with distal sequences. Regions of interest were amplified from purified genomic DNA from Kasumi-1 cells. Transient transfections of RAW264.7 cells were conducted using the Lipofectamine 2000 Reagent (Invitrogen, Paisley, UK) according to the manufacturer's protocol. Luciferase assays were performed using a dual-luciferase reporter assay system (Promega).

Expression arrays

Total RNA was labeled and hybridized to the Illumina HT-12 v4 BeadChip (Illumina).

Identification of DNaseI- and ChIP-sequencing peaks

The raw sequence data were aligned to the hg18 assembly (NCBI Build 36.1) using BWA,[29] and data were displayed using the UCSC Genome Browser.[30] Regions of enrichment of DNaseI and ChIP data were identified using MACS software.[31] *De novo* motif analysis was performed using HOMER.[32]

Microarray gene expression data analysis

Microarray gene expression data were analyzed in GenomeStudio software (Illumina) with background subtraction. The raw data output was analyzed using the Lumi R package[33] with quantile normalization. The 10% threshold (*P*-value $\leqslant 0.1$) was applied to all data. Genes were selected with at least twofold change in expression.

Gene set enrichment analysis (GSEA) was performed using the stand-alone application (Broad Institute) by ranking genes according to their correlation (Pearson) with the F1 metagene, the metagene highly expressed in the cells treated with siRNA for *RUNX1/ETO*. David/EASE analysis was performed using the online tool at http:\\david.abcc.ncifcrf.gov.[34]

A more detailed description of Methods is given in Supplementary Material.

RESULTS

Identification of high-confidence binding sites for RUNX1/ETO and RUNX1 in t(8;21) cells

In order to perform a comprehensive and stringent determination of the chromatin and expression state of all genomic regions that respond to the expression of RUNX1/ETO, we employed Kasumi-1 cells, a well-studied model of t(8;21) AML.[27,35] This cell line was obtained from a patient in second relapse after chemotherapy and bone marrow transplantation, and thus represents the most aggressive form of t(8;21) AML.[35] Kasumi-1 does not express wild-type *ETO*[36] and still carries one intact *RUNX1* allele. This permits the discrimination between wild-type and translocated RUNX1 using antibodies against either the C terminus of RUNX1 recognizing only wild-type RUNX1, or the ETO moiety recognizing only the RUNX1/ETO fusion. We identified a genome-wide set of target sites for RUNX1 and RUNX1/ETO by ChIP followed by high-throughput sequencing (ChIP sequencing; Figure 1, Supplementary Figure 1). To determine how RUNX1/ETO target genes respond to loss of RUNX1/ETO binding and to evaluate the specificity of peak calling, we performed ChIP sequencing after specific RUNX1/ETO depletion using a siRNA that targets the *RUNX1/ETO* junction within the transcript as well as both a mismatch siRNA and mock transfection as controls. This knockdown model system has been extensively validated and characterized,[17,24,26,27,36-40] and routinely leads to >70% reduction of all forms of the RUNX1/ETO protein (Figure 1a). A single siRNA electroporation yielded a maximal *RUNX1/ETO* transcript knockdown after 48 h. We therefore harvested siRNA-treated cells at this time point for ChIP experiments.

To identify high-confidence RUNX1/ETO targets regions, we first selected a set of 4598 ETO ChIP peaks that were shared between mock-transfected and mismatch control-transfected cells (Figure 1b). In all, 97% of these ETO ChIP peaks disappeared after the specific knockdown of RUNX1/ETO (Figure 1b, Supplementary Table 1). We have previously shown at specific genes that RUNX1/ETO and RUNX1 bind within DNaseI hypersensitive sites (DHSs).[7] To further increase peak confidence, we therefore mapped DHSs in Kasumi-1 cells (Supplementary Table 1) and show that >75% of both the RUNX1/ETO and also RUNX1 peaks were contained within DHSs (Figures 1c and d). Annotating these peaks yielded 3633 target regions bound by RUNX1/ETO- and 6120 RUNX1-bound regions. High-confidence RUNX1/ETO peaks were located in established target genes, such as *CSF1R* and *IGFBP7* (data not shown), the transcription factor genes *NFE2, CEBPA, NOTCH1* and *PU.1* (*SPI1*), and microRNA genes including *MIR223* and the

© 2012 Macmillan Publishers Limited

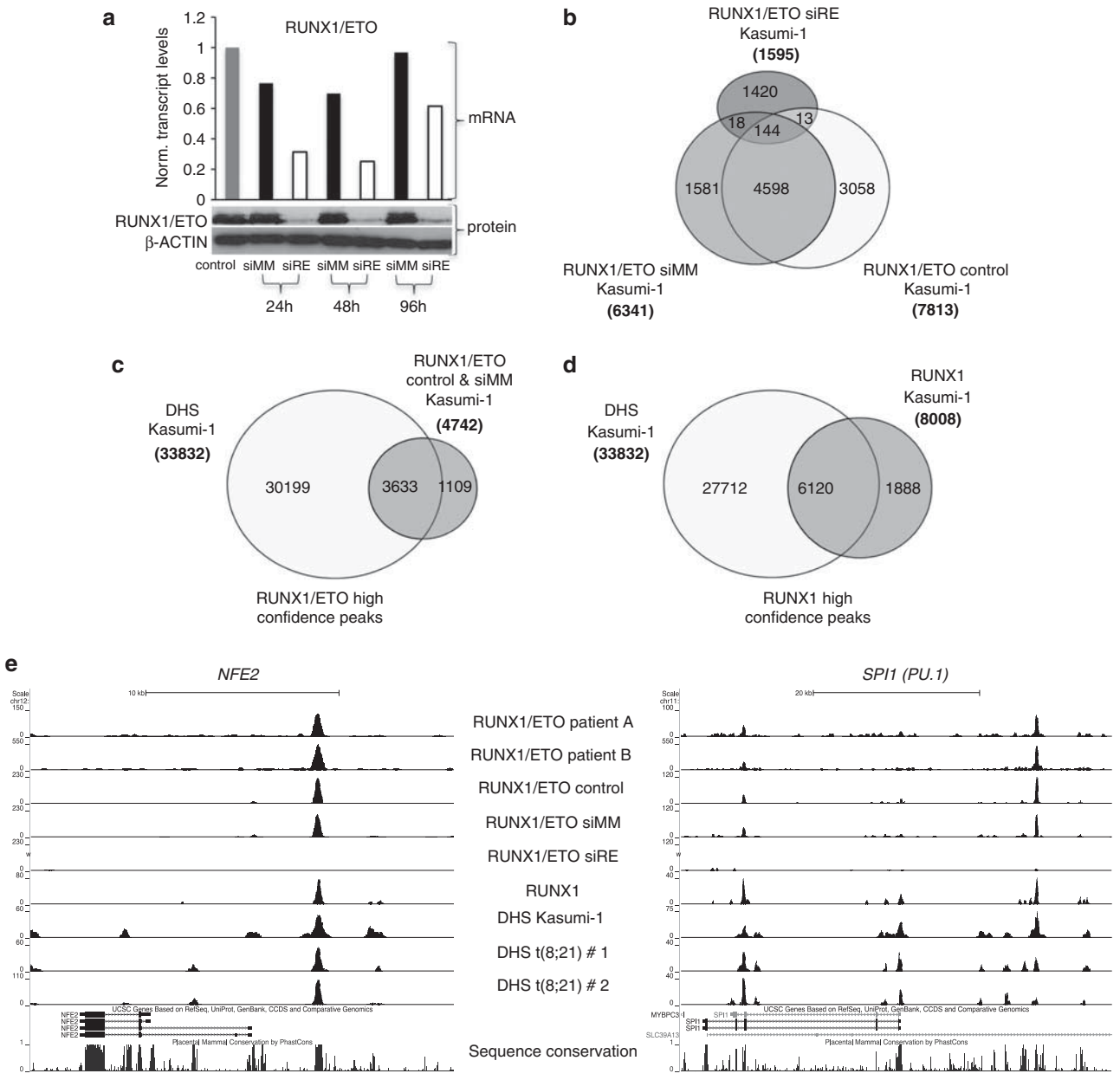

Figure 1. Identification of high-confidence binding sites for RUNX1/ETO and RUNX1. (**a**) Time course of RUNX1/ETO knockdown in Kasumi-1 cells. Top panel: real-time PCR analysis of mRNA expression; bottom panels: immunoblot detection of RUNX1/ETO protein. β-ACTIN served as loading control. Time points are indicated at the bottom. *RUNX1/ETO* transcript levels are recovering 48 h after siRNA electroporation, whereas protein levels remain low for another 24 h. siRE, RUNX1/ETO siRNA; siMM, mismatch siRNA; control, mock-transfected cells. (**b**) Intersection analysis of RUNX1/ETO peaks. The Venn diagram shows the overlap between RUNX1/ETO peaks in mock, mismatch siRNA or RUNX1/ETO siRNA-treated Kasumi-1 cells. The vast majority of RUNX1/ETO peaks were common to mock and siMM-treated Kasumi-1 cells, and >97% of the common peaks disappeared after RUNX1/ETO depletion. (**c**, **d**) Identification of high-confidence peaks for RUNX1/ETO and RUNX1 in Kasumi-1 cells. More than 75% of both the RUNX1/ETO and RUNX1 peaks colocalize with DHS in Kasumi-1 cells, thus constituting high-confidence peaks. (**e**) UCSC Genome Browser image depicting the human *NFE2* and *SPI1 (PU.1)* loci demonstrating a colocalization of RUNX1/ETO peaks in patient cells, specific RUNX1/ETO and RUNX1 peaks in Kasumi-1 cells as well as DHS.

MIR23A–27A–24-2 cluster[41] (Figure 1e, Supplementary Figure 1A). High-confidence peaks were also found between the telomerase protein gene *TERT* and *CLPTM1L*, a locus associated with several types of cancer[42] (Supplementary Figure 1A, Supplementary Table 4). Selected peaks were validated manually in Kasumi-1 cells (Supplementary Figures 1B and C) and in primary cells from a t(8;21) AML patient (Supplementary Figures 1D–F), with and without RUNX1/ETO knockdown.

To validate our genome-wide cell line ChIP-sequencing data, we compared the RUNX1/ETO-binding pattern of Kasumi-1 cells to that of primary, patient-derived t(8;21) AML cells. As with t(8;21) cell lines, the wild-type ETO protein is neither expressed in t(8;21)-negative nor in t(8;21)-positive AML cells,[36,43,44] which agrees with a lack of DHSs at the *ETO* (*RUNX1T1*) locus in all hematopoietic cell types studied here (data not shown). With primary cells from two patients (patients A and B), we obtained a large number of small peaks, many of which disappeared when analyzed at higher stringency (data not shown), but 2629 peaks occurred in both patients. In all, 76% of joint peaks intersected with DHS from the two other t(8;21) patients (no. 1 and no. 2, Supplementary Figure

© 2012 Macmillan Publishers Limited

1G, Supplementary Table 1) and thus represented high-confidence peaks. More than 50% of genes bound by RUNX1/ETO in Kasumi-1 cells were also specifically bound in patient cells (Supplementary Table 5). This high degree of concordance was also confirmed by comparing RUNX1/ETO binding to specific genes across the genome (Figure 1e, Supplementary Figure 1A), including known targets of RUNX1/ETO such as *LAT2*.[45]

RUNX1/ETO- and RUNX1-binding sites overlap only partially in t(8;21) cells

Both RUNX1 and RUNX1/ETO showed a similar pattern of distribution of binding sites for the subsets of peaks located within 1.5 kb of transcription start sites, and 60% of the RUNX1/ETO peaks overlapped with RUNX1 peaks (Figures 2a and b). The unbiased *de novo* identification of enriched consensus binding motifs showed that, in contrast to RUNX1-unique peaks, both RUNX1/ETO-associated and RUNX1/ETO-unique peaks were enriched in motifs for E-box-binding proteins (Figure 2c), in agreement with observations that these factors form stable interactions with the NHR1 domain of RUNX1/ETO.[12] The same motifs were found when examining the entire set of RUNX1- or RUNX1/ETO-bound sequences in Kasumi-1 cells (Supplementary Figures 2A and B). Both RUNX1/ETO- and RUNX1-binding regions were enriched for RUNX1 consensus sequences, but only 30% of RUNX1-unique peaks contained such motifs, indicating that at

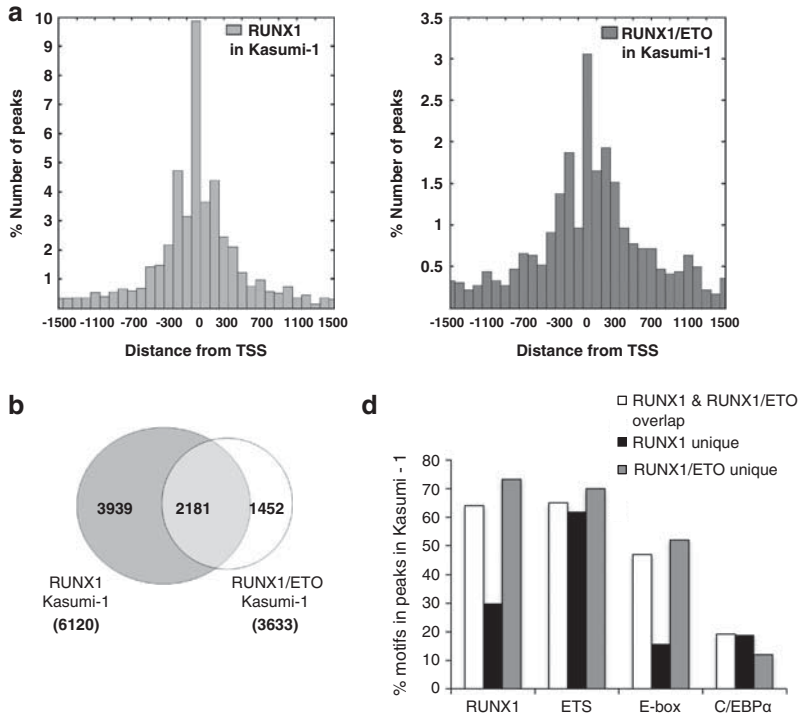

c

Motifs associated with shared RUNX1/ETO and RUNX1 peaks in Kasumi-1

motif	match	score (log p-value)
	RUNX	-1318
	ETS	-1302
	ETS	-1158
	RUNX	-567
	ETS: E-box	-437

Motifs associated with RUNX1 unique peaks in Kasumi-1

motif	match	score (log p-value)
	ETS	-1769
	ETS	-1638
	ETS	-1538
	ETS	-1418
	RUNX	-1139
	RUNX	-1111
	RUNX	-948
	C/EBP	-314

Motifs associated with RUNX1/ETO unique peaks in Kasumi-1

motif	match	score (log p-value)
	RUNX	-835
	ETS	-682
	ETS	-602
	E-box	-489
	E-box	-488
	E-box	-447
	ETS	-224

Figure 2. Identification and characterization of RUNX1/ETO and RUNX1 target regions in t(8;21) cells. (**a**) Positional distribution of RUNX1- (left) or RUNX1/ETO- (right) binding sites relative to the transcription start site (TSS) of their nearest gene. (**b**) Intersection of RUNX1 and RUNX1/ETO peaks in Kasumi-1 cells. The Venn diagram shows the numbers of high-confidence peaks bound by RUNX1 and RUNX1/ETO. (**c**) *De novo* motif discovery performed on the set of regions bound by the RUNX1 and/or RUNX1/ETO in Kasumi-1 cells identified enriched RUNX consensus and different types of ETS factor-binding sites. E-box motifs were significantly enriched in peaks either unique for RUNX1/ETO or common to RUNX1/ETO and RUNX1. (**d**) RUNX, ETS, E-box and C/EBP consensus sequence were mapped back to all regions bound by RUNX1/ETO and RUNX1. A large proportion of regions bound by RUNX1 did not contain RUNX (TGYGGT) and/or E-box (CANNTG) consensus binding motifs, whereas most regions contain ETS (GGAW) sites.

© 2012 Macmillan Publishers Limited

sites not occupied by RUNX1/ETO, RUNX1 may bind via interaction with other transcription factors. These are likely to be ETS family members, which present the top-scoring motif in this peak population (Figure 2c). In contrast, up to 70% of shared and unique RUNX1/ETO-bound sequences contained a RUNX1 motif (Figure 2d), suggesting that the fusion protein needs to

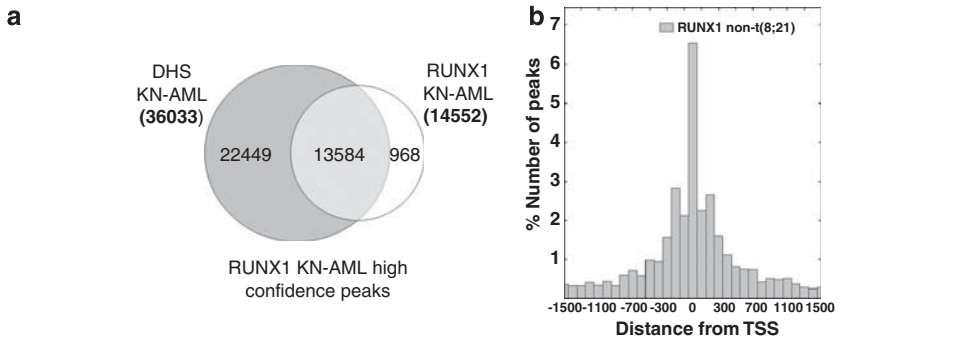

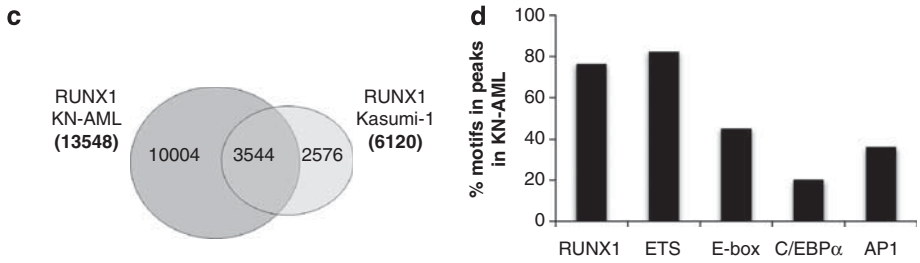

e Motifs associated with RUNX1 peaks unique to KN-AML

motif	match	score (log p-value)
	RUNX1	-4786
	ETS	-4072
	ETS	-3158
	AP1	-2320
	E-box	-1806
	CEBP	-651
	AP1	-487
	NF-kB	-480
	CEBP	-435
	NF-kB	-319

Motifs associated with RUNX1 peaks common to t(8;21) and KN-AML

motif	match	score (log p-value)
	ETS	-1978
	RUNX1	-1809
	E-box	-98

Motifs associated with RUNX1 peaks unique to t(8;21)

motif	match	score (log p-value)
	PU.1/ETS	-1084
	ETS	-1043
	PU.1/ETS	-964
	ETS	-916
	RUNX1	-804
	ETS	-224

Figure 3. RUNX1 in t(8;21)-positive and -negative leukemic cells associates with different binding sites motifs. (**a**) Identification of high-confidence RUNX1 peaks from blasts from a AML patient with a normal karyotype (KN-AML). Venn diagram showing the intersection of RUNX1 peaks with DHS. (**b**) Positional distribution of RUNX1-binding sites in KN-AML blasts relative to the transcription start site (TSS) of their nearest gene. (**c**) Intersection of RUNX1 peaks in KN-AML cells and in Kasumi-1 cells. The Venn diagram shows the numbers of high-confidence peaks bound by RUNX1. (**d**) RUNX1 consensus sequences were mapped back to all regions bound by RUNX1 in t(8;21)-negative AML blasts. A large proportion of regions exclusively bound by RUNX1 contain RUNX, ETS and E-box consensus binding motifs as well as consensus binding motifs for C/EBP and AP1. (**e**) *De novo* motif discovery performed on the set of regions bound by RUNX1 in t(8;21)-negative KN-AML blasts identifies enriched RUNX and ETS consensus sequences as well as E-box, AP1- and C/EBP-binding sites.

© 2012 Macmillan Publishers Limited

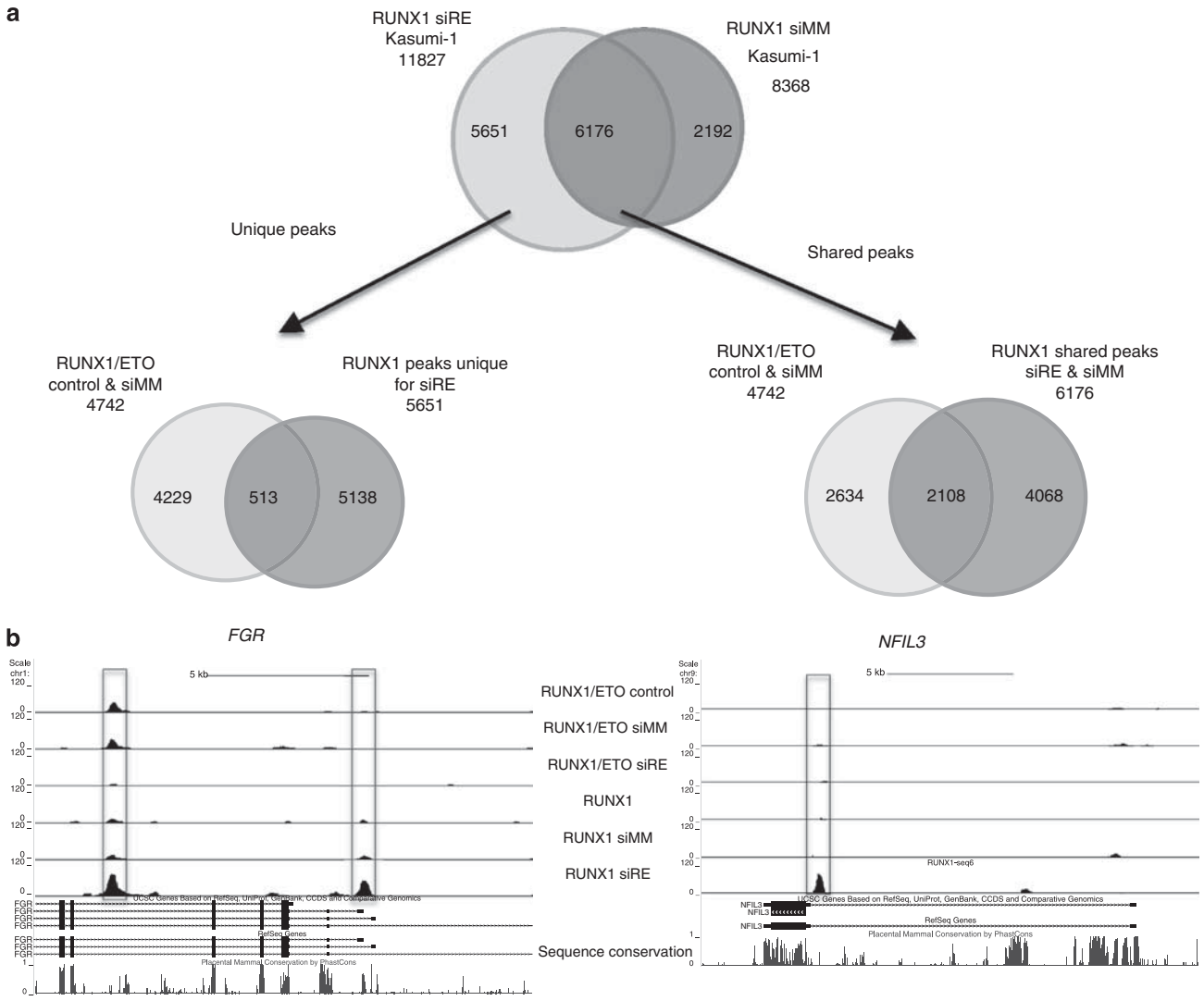

Figure 4. Knockdown of RUNX1/ETO leads to a redistribution of RUNX1 binding. Kasumi-1 cells were electroporated with either mismatch control siRNA (siMM) or RUNX1/ETO siRNA (siRE). Two days after siRNA electroporation, RUNX1 binding was measured by ChIP sequencing in both populations. (**a**) Top panel: Venn diagram showing the appearance of new RUNX1-binding sites after RUNX1/ETO depletion. Bottom left: Venn diagram showing the overlap between RUNX1/ETO-bound regions and *de novo* RUNX1 sites, demonstrating that the latter are distinct from sites previously bound by RUNX1/EO. Bottom right: Venn diagram showing the overlap between RUNX1/ETO-bound sequences and sites bound by RUNX1 before and after RUNX1/ETO depletion. (**b**) Example of alterations in RUNX1 binding. Left panel shows UCSC browser images depicting one gene (*NFIL3*) at a site not previously bound by RUNX1/ETO and another gene (*FGR)* showing a *de novo* RUNX1 with a RUNX1/ETO-bound site showing an increase in RUNX1 binding at this site after knockdown.

Figure 5. Analysis of RUNX1/ETO-dependent gene expression patterns. (**a**) Hierarchical clustering of genes responding by an at least twofold change in expression levels to RUNX1/ETO knockdown in Kasumi-1 cells. The heat map shows early upregulated (Group I), downregulated (Group II) and late upregulated genes (Group III) over a time course of 10 days. At the bottom of the heat map note non-clustered genes that are either upregulated more than threefold or show a more complex response pattern (Group IV). Expression levels were compared between RUNX1/ETO siRNA and mismatch siRNA-treated cells. Time points are indicated on the top of the heat map. Dark red indicates highly upregulated genes and black indicates highly downregulated genes. (**b**) Effect of RUNX1/ETO depletion on gene expression in primary t(8;21) AML blasts. The graph shows real-time PCR-based validation of early responding genes. The columns represent the means for three t(8;21) AML patients and the error bars the s.e.m. Inset: immunoblot showing siRNA-mediated depletion of RUNX1/ETO in blasts from a t(8;21) AML patient. (**c**) GSEA ranked according to the correlation of genes with a metagene (F1) summarizing the gene expression profile of Kasumi-1 cells after RUNX1/ETO knockdown. From left to right: significant enrichment of gene sets downregulated in human hematopoietic stem cells upon RUNX1/ETO overexpression[6] and enrichment of genes determined in this study to have a high-confidence RUNX1/ETO-binding site with a corresponding DHS in the region 2 kb upstream of the start of transcription in Kasumi-1 cells. *P*, nominal *P*-value; *q*, false discovery rate. (**d**) The numbers of upregulated and downregulated genes upon RUNX1/ETO depletion in Kasumi-1 cells. The bottom row indicates genes with RUNX1/ETO peaks. (**e**) Classification of RUNX1/ETO target genes. The columns show the percentage of genes with high-confidence RUNX1/ETO peaks of all genes with changed gene expression upon RUNX1/ETO knockdown. siMM, mismatch siRNA; siRE, RUNX1/ETO siRNA.

© 2012 Macmillan Publishers Limited

be recruited by directly anchoring it to DNA. These results contrast to recently published findings by Maiques-Diaz *et al.*,[46] who reported a substantially lower fraction of RUNX1 motifs in RUNX1/ETO peaks. This discrepancy may be due to the fact that in these experiments a ChIP-chip proximal promoter array was used.

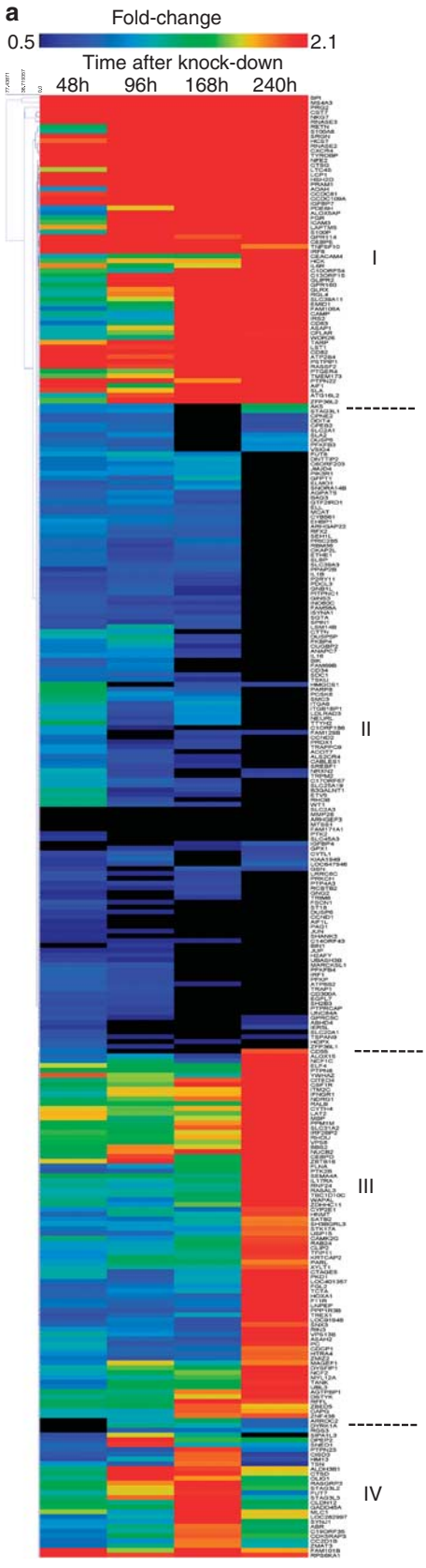

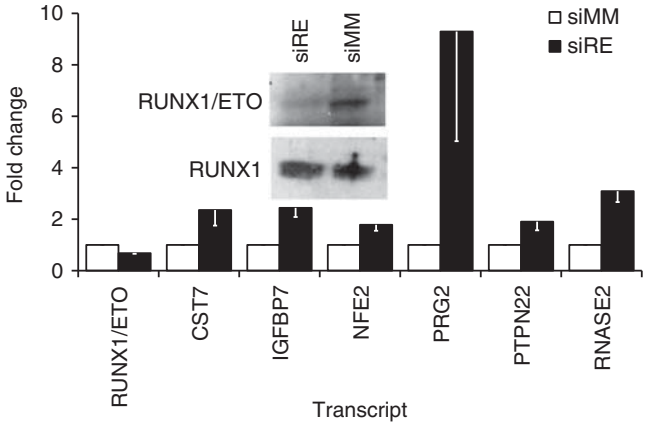

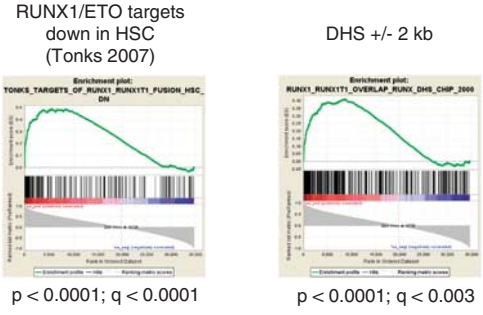

d

Time (h)	48		96		168		240	
Regulation	up	down	up	down	up	down	up	down
Total	90	68	174	106	293	256	656	741
Direct RUNX1/ETO targets	46	13	63	27	106	57	152	112

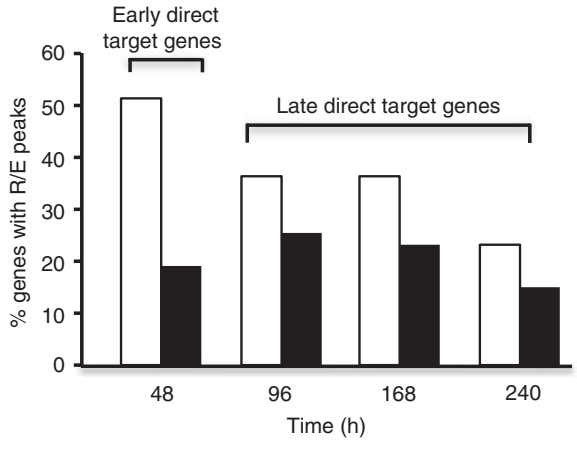

© 2012 Macmillan Publishers Limited

Differential binding of RUNX1 in AML cells without a CBF complex mutation

The incomplete overlap between RUNX1 and RUNX1/ETO peaks prompted us to investigate whether RUNX1 bound to different sequences in the human genome in RUNX1/ETO-expressing cells compared to AML cells without CBF mutations. To this end we identified genome-wide high-confidence RUNX1-binding sites in AML cells with a normal karyotype (KN-AML) from a patient that expressed a full-length RUNX1 protein (data not shown) but displayed a block at a similar differentiation stage as the t(8;21) patients and had a surface marker expression profile highly similar to the two t(8;21) AML samples (Supplementary Table 2). Similar to Kasumi-1 cells, 90% of all RUNX1 peaks in the KN-AML blast cells colocalized with DHSs (Figure 3a). Direct RUNX1 targets included genes controlling hematopoietic differentiation such as *CSF1R*, *LAT2*, and *LMO2* (Supplementary Figure 3). The KN-AML RUNX1 peaks showed a similar pattern of distribution around the transcription start sites as the RUNX1 peaks from Kasumi-1 cells (Figure 3b), but their genome-wide distribution and enriched motif composition was strikingly different. When directly compared (Figure 3c), only 26% of the KN-AML RUNX1-binding sites were found in Kasumi-1 cells. *GATA3, GCHFR* and *KLF13* are examples for this notion (Supplementary Figure 3). Most importantly, in contrast to t(8;21) cells, the RUNX1 peaks unique for KN-AML showed a highly significant enrichment for binding sites for inducible factors such as AP1, C/EBP and NF-κB (Figures 3d and e).

RUNX1/ETO knockdown leads to a shift in the pattern of RUNX1 occupancy

Our RUNX1 ChIP data indicate that the genome of hematopoietic precursor cells contains a large number of functional RUNX1-binding sites which are differentially occupied in t(8;21) AML and KN-AML cells and are associated with different binding site motifs. We therefore tested by ChIP sequencing whether depletion of RUNX1/ETO led to an alteration of RUNX1 occupancy in RUNX1/ETO expressing cells (Figure 4). The comparison between RUNX1 binding before and after knockdown showed that the depletion of RUNX1/ETO led not only to an increase in the number of RUNX1 peaks, but also to the formation of a large number of *de novo* RUNX1-binding sites (Figure 4a), as exemplified by the transcription factor gene *NFIL3*, which is upregulated by RUNX1/ETO depletion (Figure 4b, right panel). Only 10% of *de novo* peaks overlapped with RUNX1/ETO-bound sites (Figure 4a, bottom left). In contrast, a much larger proportion (34%) of peaks shared between knockdown and control samples were originally bound by RUNX1/ETO (Figure 4a, bottom right). Interestingly, although at most tested target regions depletion of RUNX1/ETO led to an upregulation of RUNX1 binding and gene expression (an example of this is shown with another upregulated gene, *FGR*, a member of the *SRC* kinase family, in Figure 4b, left panel), this was not always the case (Supplementary Figure 4). For instance, *PU.1* (*SPI1*) represents a class of genes, where RUNX1/ETO binding did not or only marginally affect RUNX1 occupancy. The *PU.1* upstream regulatory element contains an upstream enhancer element (*PU.1 (E)*) that is bound by RUNX1 at multiple sites, and this binding is vital for enhancer activity,[47] but it is also bound by RUNX1/ETO (this study). At this element RUNX1 binding did not respond to RUNX1/ETO knockdown, and gene expression was barely altered, which may indicate a complex binding pattern with multiple occupancies of both RUNX1/ETO and RUNX1.

RUNX1/ETO depletion can lead to both activation and repression of its direct target genes

In order to examine the effects of RUNX1/ETO depletion on gene expression at the global level and to correlate these changes with identified RUNX1/ETO target genes, we generated expression profiles during a time course of sustained RUNX1/ETO knockdown for 10 days in Kasumi-1 cells (Figure 5, Supplementary Table 6, Supplementary Figure 5A). Hierarchical clustering identified four groups of genes differentially responding to knockdown, consisting of early (Group I) and late (Group III) upregulated genes, downregulated genes (Group II) as well as genes showing a complex pattern of response (Group IV; Figure 5a). These results were validated by manual analysis with a selection of early responding genes both in Kasumi-1 cells and in primary t(8,21) cells obtained from three different AML patients (Figure 5b, Supplementary Figure 5B).

To compare global gene expression profiles, we produced two coordinately regulated metagenes F1 and F2 in an unsupervised manner that summarized the expression of RUNX1/ETO-dependent genes in a single score using non-negative matrix factorization.[48,49] The F1 and F2 metagenes were highly expressed in Kasumi-1 cells with and without RUNX1/ETO knockdown, respectively. We also tested the relevance of the RUNX1/ETO-dependent global gene expression changes for another t(8;21)-positive cell line, SKNO-1, and for primary t(8;21)-positive AML. Kasumi-1-derived RUNX1/ETO-dependent metagene expression was mirrored and validated in the SKNO-1 and primary AML data sets, demonstrating an excellent concordance between the RUNX1/ETO-associated global gene expression changes in these three different t(8;21)-positive cell types (Supplementary Figure 5C). Furthermore, RUNX/ETO-associated gene expression changes inversely correlated with gene expression changes observed in previous knockdown studies and in overexpression studies with primary human CD34+ cells (Figure 5c, Supplementary Figures 5D and E).[6,27,39] These combined analyses confirmed that RUNX1/ETO-associated shifts in gene expression in Kasumi-1 faithfully reflect gene expression features in the human t(8;21) AML.

The metagene was also used to rank genes for the purpose of GSEA according to their correlation with the metagene score (Supplementary Table 7). Genes with high-confidence RUNX1/ETO peaks were highly enriched in the RUNX1/ETO knockdown signature (Figure 5c). However, not all genes responding to RUNX1/ETO knockdown were associated with RUNX1/ETO peaks. Genes responding early at day 2, such as *CST7, IGFBP7* and *MTSS1*, consisted of 50% direct RUNX1/ETO target genes, whereas this was true for only 20% of the late responding genes at day 10 (Figures 5d and e). Moreover, almost 80% of all early responding target genes were upregulated upon RUNX1/ETO knockdown, in contrast to 60% of all late responding target genes (Figures 5d and e). This indicates that downstream effects of the removal of RUNX1/ETO contribute rapidly and progressively to the reorganization of the transcriptional network.

The depletion of RUNX1/ETO leads to complex changes in the histone acetylation pattern and RNA Polymerase II occupancy

As RUNX1/ETO recruits histone deacetylases to its target promoters[13,14] and alters gene transcription, we examined the immediate consequences of RUNX1/ETO depletion on histone H3 lysine 9 acetylation (H3K9Ac) and occupancy of the elongating form of RNA Polymerase II (RNA Pol II). We therefore performed ChIP experiments with RUNX1/ETO-depleted and -control cells at day 2 after knockdown, and integrated RNA Pol II and H3K9Ac data in Kasumi-1 cells on RUNX1/ETO target loci with the gene expression data (Figures 6a and b, Supplementary Table 6). After 2 days of knockdown, half of the early upregulated genes, including *IGFBP7*, *NFE2* and *PRG2*, exhibited more than twofold increased RNA Pol II occupancy, whereas most downregulated genes such as *CD34* and 75% of the late upregulated genes generally showed no or little change in RNA Pol II binding at this stage (Supplementary Figure 6A).

A more complex pattern of changes at RUNX1/ETO peaks was seen when measuring H3K9Ac. Although after 2 days of knockdown most upregulated genes displayed a rapid increase in H3K9Ac, we also found an increase at 50% of the downregulated

© 2012 Macmillan Publishers Limited

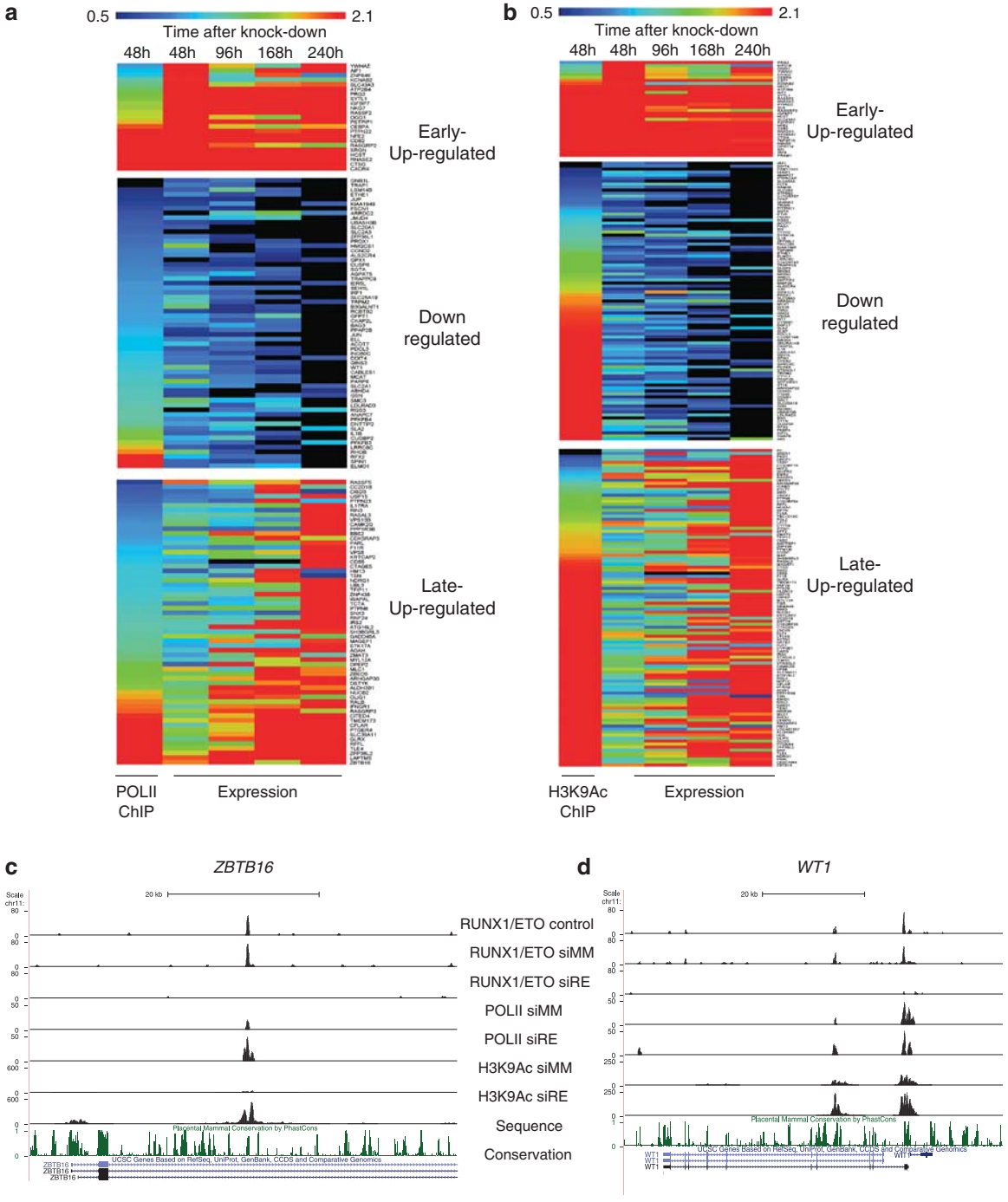

Figure 6. RUNX1/ETO silencing leads to changes in RNA-Polymerase II occupancy and the histone H3K9 acetylation pattern at RUNX1/ETO target genes. (**a**) Comparison of RNA Pol II occupation with transcriptional profiling reveals a substantial correlation between changes in gene expression and changes in RNA Pol II association upon RUNX1/ETO knockdown. RNA Pol II occupation was analyzed 48 h after siRNA treatment, ranked according to fold change in occupancy and compared with changes in gene expression during a time course of 10 days with siRNA treatment. Dark red indicates high occupancy or upregulation, black low occupancy or downregulation, respectively. (**b**) The H3K9Ac pattern correlates partially with changes in gene expression associated with RUNX1/ETO depletion. H3K9Ac occupation was analyzed and compared analogously to (**a**). (**c**, **d**) UCSC Genome Browser image of the human *ZBTB16* and *WT1* loci depicting ChIP-Seq tags for RUNX1/ETO, RNA-Pol II and H3K9Ac in mock-treated (control), mismatch siRNA (siMM) and RUNX1/ETO siRNA (siRE)-treated Kasumi-1 cells. (**e**) Heat map resulting from an unsupervised clustering of H3K9Ac- and RUNX1/ETO-binding sites with and without RUNX1/ETO knockdown (siMM and siRE, respectively) as well as without transfection (control) showing two groups of sequences and their genomic location. In each lane, the ChIP enrichment score is shown 10 kb upstream and downstream from the peak center. (**f**) Integration of the sequence enrichment of each group into a density plot showing the location of RUNX1/ETO-binding sites with and without knockdown in relation to H3K9Ac. Dark blue: H3K9Ac (siMM); pink: H3K9Ac (siRE); green: RUNX1/ETO (control); yellow RUNX1/ETO (siMM); light blue: RUNX1/ETO (siRE).

© 2012 Macmillan Publishers Limited

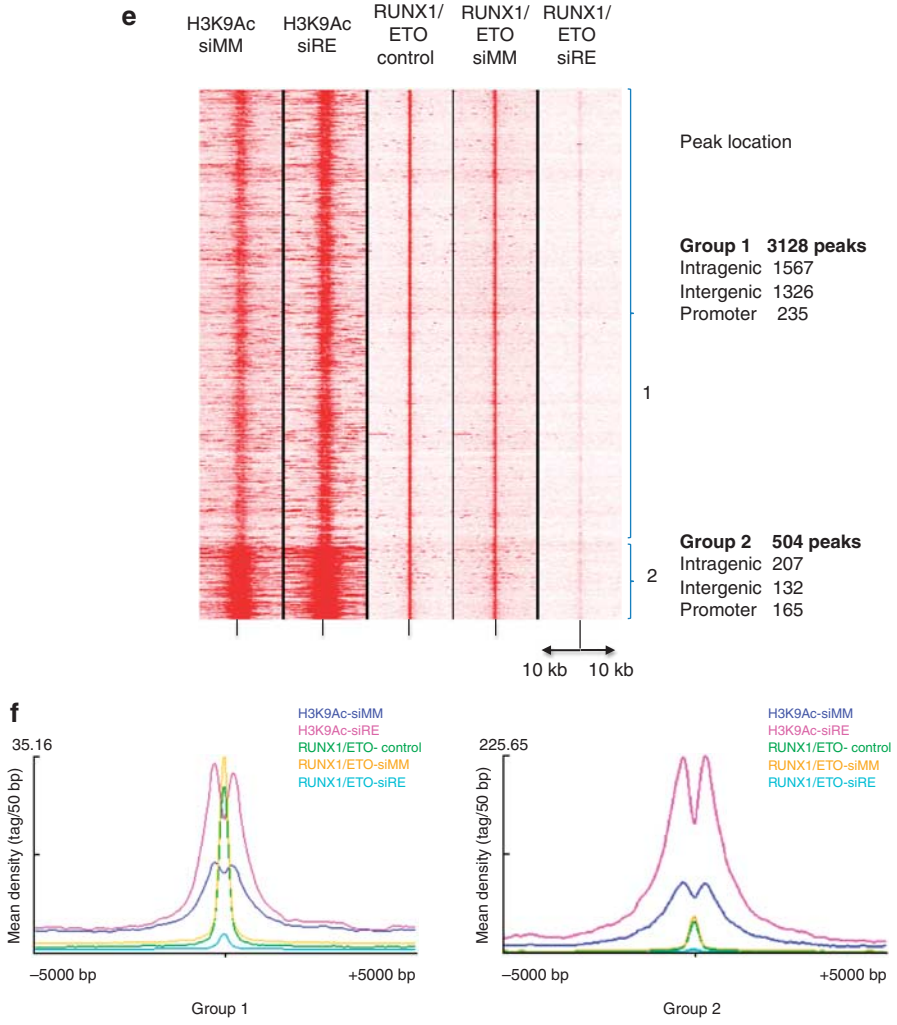

Figure 6. Continued.

genes (Figure 6b). This group of down-regulated genes partially overlapped with genes displaying an increase in RNA Pol II occupancy (Figure 6a, Supplementary Figures 6B and C). Such peaks were often localized in introns (for example, *ZBTB16* or *WT1*, Figures 6c and d) indicating that not all RUNX1/ETO peaks that are associated with alterations of gene expression colocalize with classical promoter or enhancer elements. This diversity was also reflected in reporter gene assays of the promoters of target genes (Supplementary Figure 6D): Many, but not all, of these promoter elements directly responded to transactivation by RUNX1 and repression by RUNX1/ETO.

We next used our histone acetylation data to examine the chromatin architecture and the genomic distribution of RUNX1/ETO-binding sites (Figures 6e and f). Unsupervised clustering showed that RUNX1/ETO-binding sites could be clustered into two groups (Figure 6e). The largest group contained intergenic and intragenic sites that are most likely to be enhancers, as these elements are also DNase I hypersensitive. The analysis of the histone H3K9 acetylation profile before and after knockdown (Figure 6f) showed that in both groups the RUNX1/ETO complex was flanked by acetylated histones, demonstrating that histone acetylation was not absent in such elements. This is consistent with findings that described the presence of histone acetyl transferases at these sites.[7,20] However, the depletion of RUNX1/ETO led to a strong increase in H3K9Ac, while maintaining a protein complex between nucleosomes, demonstrating that RUNX1/ETO does not lead to the formation of inactive chromatin, but shifts the balance between active and inactive chromatin.

RUNX1/ETO depletion induces myeloid differentiation and silences leukemic self-renewal programs

Finally, we asked which pathways and transcriptional programs responded to regulation by RUNX1/ETO. Functional annotation clustering separated RUNX1/ETO-bound genes from those exclusively bound by RUNX1. In both primary cells and cell lines, genes bound by the fusion protein are involved in processes, such as cytoskeletal organization, cell adhesion and cell cycle control, whereas genes solely bound by RUNX1 cluster with genes for nuclear structures, translation-associated processes and RNA processing (Supplementary Table 8). Genes responding to RUNX1/ETO knockdown showed a link with cytoskeleton, cell adhesion and migration, similar to those containing high-confidence RUNX1/ETO peaks (Supplementary Table 8). Moreover, separate analysis for upregulated and downregulated genes suggested an association of upregulated genes with differentiation, whereas downregulated genes are involved in proliferation and cell cycle regulation (Supplementary Table 9). These combined analyses suggest that the downregulated RUNX1/ETO genes are preferentially involved in proliferation and cell cycle progression, whereas upregulated genes are involved in myeloid differentiation. Indeed, suppression of RUNX1/ETO in t(8;21) AML

© 2012 Macmillan Publishers Limited

cell lines impairs clonogenicity and proliferation, and leads to cell cycle arrest in G1 phase.[26]

This notion is further supported by gene expression profile comparison and GSEA. Metagene-based comparison with global gene expression profiles from cells of different normal human hematopoietic differentiation stages[50] demonstrate that Kasumi-1 cells depleted for RUNX1/ETO change their combined gene expression pattern from a unique specific subset remotely related to lymphoid and early myeloid precursors towards that of the normal granulocyte/monocyte precursor, monocyte and neutrophil subsets (Figure 7a).

GSEA showed that knockdown of RUNX1/ETO resulted in significant downregulation of cell cycle progression, telomere maintenance genes and TERT target genes (Figure 7b, Supplementary Figure 7A, Supplementary Table 7). In particular, the inverse correlation between RUNX1/ETO knockdown and TERT target gene expression supports a model of RUNX1/ETO-controlled telomerase activity, a key factor of normal and malignant self-renewal.[37] In both t(8;21)-positive Kasumi-1 and patient-derived primary AML cells, RUNX1/ETO binds to a region between *TERT* and *CLPTM1L* implying *TERT* as a direct target gene of RUNX1/ETO (Supplementary Figure 1A). Indeed, sustained suppression of *RUNX1/ETO* caused an increasingly pronounced inhibition of *TERT* expression over time in Kasumi-1 and in SKNO-1 cells (Figure 7c, Supplementary Figure 7B). Interestingly, in spite of being highly activated particularly in *MLL*-rearranged leukemias, *HOXB* and late *HOXA* genes may not be part of the RUNX1/ETO-driven self-renewal program.[51] In both t(8;21)-positive cell lines and AML blasts, several *HOXA* members including *HOXA9* as well as the complete *HOXB* locus showed low or absent expression levels and a lack of DHSs (Supplementary Figure 7C).

DISCUSSION

Gain-of-function studies using ectopic expression of RUNX1/ETO in t(8;21)-negative leukemic and non-leukemic cells have yielded

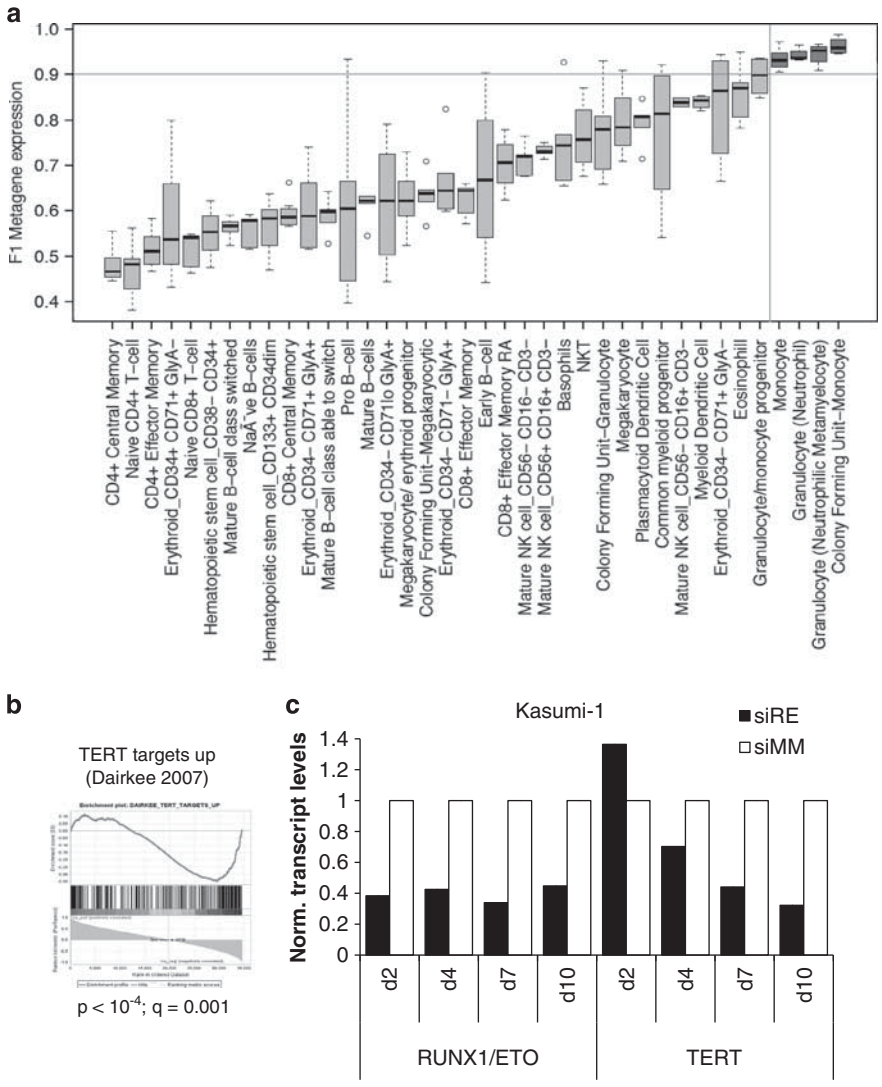

Figure 7. RUNX1/ETO knockdown interferes with leukemic self-renewal and promotes myeloid differentiation. (**a**) Comparison of F1 metagene expression in normal hematopoietic sub-populations[50] reveals high similarity between gene expression patterns of RUNX1/ETO-depleted Kasumi-1 cells and those of monocytic and granulocytic cell types. The values of the F1 metagene for siMM-treated and siRE-treated Kasumi-1 cells are close to 0 and 1, respectively. Those colored red are cell types for which expression of the metagene is at least equal to RUNX1/ETO-depleted Kasumi-1 cells indicating maximum similarity. (**b**) Gene set enrichment analysis using a ranking of TERT targets and their correlation with the F1 metagene showing an inverse correlation of expression after knockdown.[60] *P*, nominal *P*-value; *q*, false discovery rate. (**c**) RUNX1/ETO depletion inhibits *TERT* expression. t(8;21)-positive Kasumi-1 were electroporated with either RUNX1/ETO or mismatch siRNA (siRE and siMM, respectively) at day 2, 4, 7 and 10. *RUNX1/ETO* and *TERT* transcript levels were analyzed at the indicated time points by real-time PCR. The color reproduction of this figure is available at the *Leukemia* journal online.

© 2012 Macmillan Publishers Limited

insights into the molecular mechanisms of initiating leukemogenesis,[6,46,52-54] whereas loss of function studies in actual leukemic t(8;21) cells (including the Kasumi-1 cells described here) inform about the role of RUNX1/ETO in maintaining leukemia.[24,25,36,39] Our experiments and novel integrative data analyses demonstrate a substantial concordance between these two approaches, indicating that integral parts of the t(8;21)-specific leukemia-initiating program are also required for maintaining the leukemic phenotype. In both primary cells and cell lines, RUNX1/ETO binds genes associated with the control of the cell cycle and cell structure. Concordantly, siRNA-mediated depletion of RUNX1/ETO affects transcriptional programs associated with myeloid differentiation, proliferation and self-renewal, in addition to those promoting cell cycle progression and DNA synthesis.

Our siRNA knockdown shows that RUNX1/ETO binding leads to large-scale, but reversible, alterations throughout the epigenome. H3K9Ac at RUNX1/ETO-binding sites was mostly increased after knockdown, which is consistent with a repressive role of the fusion protein at these sites. However, RUNX1/ETO depletion was also associated with upregulation of gene expression. In a recent study, RUNX1/ETO was shown to also regulate gene activation in a p300-dependent manner.[20] Concurrent with this observation, when combined with gene expression data, RUNX1/ETO depletion concurred with strikingly complex regulatory patterns, with an increase of H3K9Ac and RNA Pol II binding alterations being associated with both upregulated and downregulated genes. An illustrative example for this notion is the *CD34* locus (Supplementary Figure 6C, lower panel), which contains an intragenic RUNX1/ETO site and is downregulated by RUNX1/ETO depletion, but shows increased histone acetylation at the main promoter. At the *WT1* locus, RUNX1/ETO binds to an element downstream of the main start site that contains a bidirectional promoter driving an alternative *WT1* transcript and an inhibitory antisense intronic transcript.[55] RUNX1/ETO may therefore maintain *WT1* expression by repressing the expression of non-coding RNAs.[55] This is of significant clinical interest because the level of *WT1* transcription is a prognostic factor in leukemia diagnosis.[56] Moreover, we also found widespread siRNA-mediated changes in H3K9Ac at RUNX1/ETO peaks that were not associated with alterations of steady-state mRNA levels. These elements may represent sites that respond to the upregulation of myeloid regulators such as C/EBPα and prime genes for the onset of myeloid differentiation. Follow-up of these observations is outside of the scope of this study, but our datasets provide a wealth of resources for experiments unravelling the mechanistic details of such changes.

Another important result from this study is our finding that the depletion of RUNX1/ETO and subsequent cell differentiation is associated with a redistribution of RUNX1-binding activity throughout the genome. We observed a large number of new binding sites distinct from those previously bound by RUNX1/ETO. The induction of myeloid differentiation after RUNX1/ETO depletion therefore involves not only loss of repression, but also increased recruitment of transcriptional activators to additional sites. Currently, we do not know how RUNX1 is directed to new sites, but it is likely that this involves the interaction of RUNX1 with other transcription factors whose activity is altered by RUNX1/ETO, such as C/EBPα and PU.1.[15,57] Our observation of a differential binding of RUNX1 is also important in the context of leukemogenesis in general because it implies that mutations of RUNX1 that are widespread in leukemogenesis and cause specific disease phenotypes may differentially affect alternate subsets of genes depending on how the interaction with cooperating transcription factors is altered at each gene.[58,59] Therefore, one of the future challenges in leukemia research will be to unravel the differential activity of transcription factors in a system-wide manner and to model the regulatory consequences of such differences for each specific type of leukemia.

In conclusion, our study demonstrates that epigenetic alterations mediated by RUNX1/ETO are reversible at a global scale by solely interfering with its function, emphasizing the feasibility of targeted therapeutic approaches either using siRNA or small molecules.

CONFLICT OF INTEREST

The authors declare no conflict of interest.

ACKNOWLEDGEMENTS

This work was funded by a specialist program grant from Leukaemia and Lymphoma Research (CB, PC, RT), grants from Yorkshire Cancer Research (PC and CB), Cancer Research UK (BDY), the NIH (NIH R01 CA118316, DGT) and Kay Kendall Leukaemia Fund (OH). We thank Berthold Gottgens (Cambridge) for helpful comments on the manuscript.

REFERENCES

1 Bonifer C, Bowen DT. Epigenetic mechanisms regulating normal and malignant haematopoiesis: new therapeutic targets for clinical medicine. *Expert Rev Mol Med* 2010; **12**: e6.
2 Wang Q, Stacy T, Miller JD, Lewis AF, Gu TL, Huang X *et al.* The CBFbeta subunit is essential for CBFalpha2 (AML1) function *in vivo*. *Cell* 1996; **87**: 697-708.
3 Okuda T, van Deursen J, Hiebert SW, Grosveld G, Downing JR. AML1, the target of multiple chromosomal translocations in human leukemia, is essential for normal fetal liver hematopoiesis. *Cell* 1996; **84**: 321-330.
4 Erickson P, Gao J, Chang KS, Look T, Whisenant E, Raimondi S *et al.* Identification of breakpoints in t(8;21) acute myelogenous leukemia and isolation of a fusion transcript, AML1/ETO, with similarity to Drosophila segmentation gene, runt. *Blood* 1992; **80**: 1825-1831.
5 Miyoshi H, Kozu T, Shimizu K, Enomoto K, Maseki N, Kaneko Y *et al.* The t(8;21) translocation in acute myeloid leukemia results in production of an AML1-MTG8 fusion transcript. *EMBO J* 1993; **12**: 2715-2721.
6 Tonks A, Pearn L, Musson M, Gilkes A, Mills KI, Burnett AK *et al.* Transcriptional dysregulation mediated by RUNX1-RUNX1T1 in normal human progenitor cells and in acute myeloid leukaemia. *Leukemia* 2007; **21**: 2495-2505.
7 Follows GA, Tagoh H, Lefevre P, Hodge D, Morgan GJ, Bonifer C. Epigenetic consequences of AML1-ETO action at the human c-FMS locus. *EMBO J* 2003; **22**: 2798-2809.
8 Frank R, Zhang J, Uchida H, Meyers S, Hiebert SW, Nimer SD. The AML1/ETO fusion protein blocks transactivation of the GM-CSF promoter by AML1B. *Oncogene* 1995; **11**: 2667-2674.
9 Okuda T, Cai Z, Yang S, Lenny N, Lyu CJ, van Deursen JM *et al.* Expression of a knocked-in AML1-ETO leukemia gene inhibits the establishment of normal definitive hematopoiesis and directly generates dysplastic hematopoietic progenitors. *Blood* 1998; **91**: 3134-3143.
10 Yergeau DA, Hetherington CJ, Wang Q, Zhang P, Sharpe AH, Binder M *et al.* Embryonic lethality and impairment of haematopoiesis in mice heterozygous for an AML1-ETO fusion gene. *Nat Genet* 1997; **15**: 303-306.
11 Meyers S, Downing JR, Hiebert SW. Identification of AML-1 and the (8;21) translocation protein (AML-1/ETO) as sequence-specific DNA-binding proteins: the runt homology domain is required for DNA binding and protein-protein interactions. *Mol Cell Biol* 1993; **13**: 6336-6345.
12 Zhang J, Kalkum M, Yamamura S, Chait BT, Roeder RG. E protein silencing by the leukemogenic AML1-ETO fusion protein. *Science* 2004; **305**: 1286-1289.
13 Gelmetti V, Zhang J, Fanelli M, Minucci S, Pelicci PG, Lazar MA. Aberrant recruitment of the nuclear receptor corepressor-histone deacetylase complex by the acute myeloid leukemia fusion partner ETO. *Mol Cell Biol* 1998; **18**: 7185-7191.
14 Lutterbach B, Westendorf JJ, Linggi B, Patten A, Moniwa M, Davie JR *et al.* ETO, a target of t(8;21) in acute leukemia, interacts with the N-CoR and mSin3 corepressors. *Mol Cell Biol* 1998; **18**: 7176-7184.
15 Pabst T, Mueller BU, Harakawa N, Schoch C, Haferlach T, Behre G *et al.* AML1-ETO downregulates the granulocytic differentiation factor C/EBPalpha in t(8;21) myeloid leukemia. *Nat Med* 2001; **7**: 444-451.
16 Wang J, Xie LY, Allan S, Beach D, Hannon GJ. Myc activates telomerase. *Genes Dev* 1998; **12**: 1769-1774.
17 Berg T, Fliegauf M, Burger J, Staege MS, Liu S, Martinez N *et al.* Transcriptional upregulation of p21/WAF/Cip1 in myeloid leukemic blasts expressing AML1-ETO. *Haematologica* 2008; **93**: 1728-1733.
18 Peterson LF, Yan M, Zhang DE. The p21Waf1 pathway is involved in blocking leukemogenesis by the t(8;21) fusion protein AML1-ETO. *Blood* 2007; **109**: 4392-4398.

© 2012 Macmillan Publishers Limited

19 Viale A, De Franco F, Orleth A, Cambiaghi V, Giuliani V, Bossi D *et al.* Cell-cycle restriction limits DNA damage and maintains self-renewal of leukaemia stem cells. *Nature* 2009; **457**: 51 - 56.
20 Wang L, Gural A, Sun XJ, Zhao X, Perna F, Huang G *et al.* The leukemogenicity of AML1-ETO is dependent on site-specific lysine acetylation. *Science* 2011; **333**: 765 - 769.
21 Wiemels JL, Xiao Z, Buffler PA, Maia AT, Ma X, Dicks BM *et al.* In utero origin of t(8;21) AML1-ETO translocations in childhood acute myeloid leukemia. *Blood* 2002; **99**: 3801 - 3805.
22 Yuan Y, Zhou L, Miyamoto T, Iwasaki H, Harakawa N, Hetherington CJ *et al.* AML1-ETO expression is directly involved in the development of acute myeloid leukemia in the presence of additional mutations. *Proc Natl Acad Sci USA* 2001; **98**: 10398 - 10403.
23 Wang YY, Zhou GB, Yin T, Chen B, Shi JY, Liang WX *et al.* AML1-ETO and C-KIT mutation/overexpression in t(8;21) leukemia: implication in stepwise leukemogenesis and response to Gleevec. *Proc Natl Acad Sci USA* 2005; **102**: 1104 - 1109.
24 Fazi F, Zardo G, Gelmetti V, Travaglini L, Ciolfi A, Di Croce L *et al.* Heterochromatic gene repression of the retinoic acid pathway in acute myeloid leukemia. *Blood* 2007; **109**: 4432 - 4440.
25 Wichmann C, Chen L, Heinrich M, Baus D, Pfitzner E, Zornig M *et al.* Targeting the oligomerization domain of ETO interferes with RUNX1/ETO oncogenic activity in t(8;21)-positive leukemic cells. *Cancer Res* 2007; **67**: 2280 - 2289.
26 Martinez N, Drescher B, Riehle H, Cullmann C, Vornlocher HP, Ganser A *et al.* The oncogenic fusion protein RUNX1-CBFA2T1 supports proliferation and inhibits senescence in t(8;21)-positive leukaemic cells. *BMC Cancer* 2004; **4**: 44.
27 Dunne J, Cullmann C, Ritter M, Soria NM, Drescher B, Debernardi S *et al.* siRNA-mediated AML1/MTG8 depletion affects differentiation and proliferation-associated gene expression in t(8;21)-positive cell lines and primary AML blasts. *Oncogene* 2006; **25**: 6067 - 6078.
28 Leddin M, Perrod C, Hoogenkamp M, Ghani S, Assi S, Heinz S *et al.* Two distinct auto-regulatory loops operate at the PU.1 locus in B cells and myeloid cells. *Blood* 2011; **117**: 2827 - 2838.
29 Li H, Durbin R. Fast and accurate long-read alignment with Burrows-Wheeler transform. *Bioinformatics* 2010; **26**: 589 - 595.
30 Kent WJ, Sugnet CW, Furey TS, Roskin KM, Pringle TH, Zahler AM *et al.* The human genome browser at UCSC. *Genome Res* 2002; **12**: 996 - 1006.
31 Zhang Y, Liu T, Meyer CA, Eeckhoute J, Johnson DS, Bernstein BE *et al.* Model-based analysis of ChIP-Seq (MACS). *Genome Biol* 2008; **9**: R137.
32 Heinz S, Benner C, Spann N, Bertolino E, Lin YC, Laslo P *et al.* Simple combinations of lineage-determining transcription factors prime cis-regulatory elements required for macrophage and B cell identities. *Mol Cell* 2010; **38**: 576 - 589.
33 Du P, Kibbe WA, Lin SM. Lumi: a pipeline for processing Illumina microarray. *Bioinformatics* 2008; **24**: 1547 - 1548.
34 Huang da W, Sherman BT, Lempicki RA. Systematic and integrative analysis of large gene lists using DAVID bioinformatics resources. *Nat Protoc* 2009; **4**: 44 - 57.
35 Asou H, Tashiro S, Hamamoto K, Otsuji A, Kita K, Kamada N. Establishment of a human acute myeloid leukemia cell line (Kasumi-1) with 8;21 chromosome translocation. *Blood* 1991; **77**: 2031 - 2036.
36 Heidenreich O, Krauter J, Riehle H, Hadwiger P, John M, Heil G *et al.* AML1/MTG8 oncogene suppression by small interfering RNAs supports myeloid differentiation of t(8;21)-positive leukemic cells. *Blood* 2003; **101**: 3157 - 3163.
37 Gessner A, Thomas M, Castro PG, Buchler L, Scholz A, Brummendorf TH *et al.* Leukemic fusion genes MLL/AF4 and AML1/MTG8 support leukemic self-renewal by controlling expression of the telomerase subunit TERT. *Leukemia* 2010; **24**: 1751 - 1759.
38 Thomas M, Gessner A, Vornlocher HP, Hadwiger P, Greil J, Heidenreich O. Targeting MLL-AF4 with short interfering RNAs inhibits clonogenicity and engraftment of t(4;11)-positive human leukemic cells. *Blood* 2005; **106**: 3559 - 3566.
39 Corsello SM, Roti G, Ross KN, Chow KT, Galinsky I, DeAngelo DJ *et al.* Identification of AML1-ETO modulators by chemical genomics. *Blood* 2009; **113**: 6193 - 6205.
40 Martinez Soria N, Tussiwand R, Ziegler P, Manz MG, Heidenreich O. Transient depletion of RUNX1/RUNX1T1 by RNA interference delays tumour formation *in vivo*. *Leukemia* 2009; **23**: 188 - 190.
41 Zaidi SK, Dowdy CR, van Wijnen AJ, Lian JB, Raza A, Stein JL *et al.* Altered Runx1 subnuclear targeting enhances myeloid cell proliferation and blocks differentiation by activating a miR-24/MKP-7/MAPK network. *Cancer Res* 2009; **69**: 8249 - 8255.
42 Rafnar T, Sulem P, Stacey SN, Geller F, Gudmundsson J, Sigurdsson A *et al.* Sequence variants at the TERT-CLPTM1L locus associate with many cancer types. *Nat Genet* 2009; **41**: 221 - 227.
43 Ross ME, Mahfouz R, Onciu M, Liu HC, Zhou X, Song G *et al.* Gene expression profiling of pediatric acute myelogenous leukemia. *Blood* 2004; **104**: 3679 - 3687.
44 Debernardi S, Lillington DM, Chaplin T, Tomlinson S, Amess J, Rohatiner A *et al.* Genome-wide analysis of acute myeloid leukemia with normal karyotype reveals a unique pattern of homeobox gene expression distinct from those with translocation-mediated fusion events. *Genes Chromosomes Cancer* 2003; **37**: 149 - 158.
45 Duque-Afonso J, Yalcin A, Berg T, Abdelkarim M, Heidenreich O, Lubbert M. The HDAC class I-specific inhibitor entinostat (MS-275) effectively relieves epigenetic silencing of the LAT2 gene mediated by AML1/ETO. *Oncogene* 2011; **30**: 3062 - 3072.
46 Maiques-Diaz A, Chou FS, Wunderlich M, Gómez-López G, Jacinto FV, Rodriguez-Perales S *et al.* Chromatin modifications induced by the AML1-ETO fusion protein reversibly silence its genomic targets through AML1 and Sp1 binding motifs. *Leukemia* 2012; e-pub ahead of print 13 January 2012, doi:10.1038/leu.2011.376.
47 Rosenbauer F, Wagner K, Kutok JL, Iwasaki H, Le Beau MM, Okuno Y *et al.* Acute myeloid leukemia induced by graded reduction of a lineage-specific transcription factor, PU.1. *Nat Genet* 2004; **36**: 624 - 630.
48 Brunet JP, Tamayo P, Golub TR, Mesirov JP. Metagenes and molecular pattern discovery using matrix factorization. *Proc Natl Acad Sci USA* 2004; **101**: 4164 - 4169.
49 Tamayo P, Scanfeld D, Ebert BL, Gillette MA, Roberts CW, Mesirov JP. Metagene projection for cross-platform, cross-species characterization of global transcriptional states. *Proc Natl Acad Sci USA* 2007; **104**: 5959 - 5964.
50 Novershtern N, Subramanian A, Lawton LN, Mak RH, Haining WN, McConkey ME *et al.* Densely interconnected transcriptional circuits control cell states in human hematopoiesis. *Cell* 2011; **144**: 296 - 309.
51 Smith LL, Yeung J, Zeisig BB, Popov N, Huijbers I, Barnes J *et al.* Functional crosstalk between Bmi1 and MLL/Hoxa9 axis in establishment of normal hematopoietic and leukemic stem cells. *Cell Stem Cell* 2011; **8**: 649 - 662.
52 Alcalay M, Meani N, Gelmetti V, Fantozzi A, Fagioli M, Orleth A *et al.* Acute myeloid leukemia fusion proteins deregulate genes involved in stem cell maintenance and DNA repair. *J Clin Invest* 2003; **112**: 1751 - 1761.
53 Gardini A, Cesaroni M, Luzi L, Okumura AJ, Biggs JR, Minardi SP *et al.* AML1/ETO oncoprotein is directed to AML1 binding regions and co-localizes with AML1 and HEB on its targets. *PLoS Genet* 2008; **4**: e1000275.
54 Mulloy JC, Cammenga J, Berguido FJ, Wu K, Zhou P, Comenzo RL *et al.* Maintaining the self-renewal and differentiation potential of human CD34+ hematopoietic cells using a single genetic element. *Blood* 2003; **102**: 4369 - 4376.
55 Hancock AL, Brown KW, Moorwood K, Moon H, Holmgren C, Mardikar SH *et al.* A CTCF-binding silencer regulates the imprinted genes AWT1 and WT1-AS and exhibits sequential epigenetic defects during Wilms' tumourigenesis. *Hum Mol Genet* 2007; **16**: 343 - 354.
56 Bergmann L, Miething C, Maurer U, Brieger J, Karakas T, Weidmann E *et al.* High levels of Wilms' tumor gene (wt1) mRNA in acute myeloid leukemias are associated with a worse long-term outcome. *Blood* 1997; **90**: 1217 - 1225.
57 Vangala RK, Heiss-Neumann MS, Rangatia JS, Singh SM, Schoch C, Tenen DG *et al.* The myeloid master regulator transcription factor PU.1 is inactivated by AML1-ETO in t(8;21) myeloid leukemia. *Blood* 2003; **101**: 270 - 277.
58 Matheny CJ, Speck ME, Cushing PR, Zhou Y, Corpora T, Regan M *et al.* Disease mutations in RUNX1 and RUNX2 create nonfunctional, dominant-negative, or hypomorphic alleles. *EMBO J* 2007; **26**: 1163 - 1175.
59 Osato M. Point mutations in the RUNX1/AML1 gene: another actor in RUNX leukemia. *Oncogene* 2004; **23**: 4284 - 4296.
60 Dairkee SH, Nicolau M, Sayeed A, Champion S, Ji Y, Moore DH *et al.* Oxidative stress pathways highlighted in tumor cell immortalization: association with breast cancer outcome. *Oncogene* 2007; **26**: 6269 - 6279.

SOME RIGHTS RESERVED
This work is licensed under the Creative Commons Attribution-NonCommercial-No Derivative Works 3.0 Unported License. To view a copy of this license, visit http://creativecommons.org/licenses/by-nc-nd/3.0/

Supplementary Information accompanies the paper on the Leukemia website (http://www.nature.com/leu)